Application of numerical exciton-wave-function calculations to the question of band alignment in Si/$Si_{1-x}Ge_x$ quantum wells

C. Penn, F. Schäffler, and G. Bauer
Institut für Halbleiterphysik, Johannes Kepler Universität Linz, Linz, Austria

S. Glutsch
Institut für Festkörpertheorie und Theoretische Optik, Friedrich-Schiller Universität Jena, Jena, Germany

(Received 8 December 1998)

We numerically calculate the two-particle ground-state wave functions for excitons in $Si_{0.7}Ge_{0.3}$ quantum wells in an effective mass model and demonstrate how oscillator strength, binding energy, and electron distribution vary with conduction-band offset and well width. Recombination energies for the two types of excitons involving electrons in different conduction-band valleys are compared. We point out that only due to the very different electron masses in growth direction for Δ_4 and Δ_2 valleys is it possible that the Δ_2-heavy-hole exciton forms the ground state, as was reported in recent photoluminescence experiments at extremely low excitation powers [M. L. W. Thewalt *et al.*, Phys. Rev. Lett. **79**, 269 (1997)]. It is shown that those experiments can only be explained with a type-II offset for the Δ_4 conduction band of about 40 meV, in contrast to the common assumption that those data would have proven an offset of at most 10 meV for $x=0.3$. [S0163-1829(99)05019-5]

I. INTRODUCTION

Strained $Si_{1-x}Ge_x$ layers can be deposited pseudomorphically on Si by epitaxial techniques like molecular beam epitaxy (MBE) or chemical vapor deposition (CVD). This offers the possibility to build heterostructure devices on a Si basis and therefore to introduce the concept of band-gap engineering into Si technology. One example for the realization of this idea is the hetero-bipolar transistor (HBT), which is intended to rival GaAs transistors in high frequency applications. Other examples are the serious attempts to use $Si_{1-x}Ge_x$ channels for the *p*-type components of complementary metal-oxide semiconductor (CMOS) circuits.[1] In spite of this growing technological importance, the very fundamental and important property conduction-band offset still remained uncertain, with theoretical and experimental works contradicting each other even in the sign of the offset (for a review see, e.g., Ref. 2). The latest attempt to solve the problem by Thewalt *et al.*[3] involved photoluminescence under applied stress and extremely low excitation powers, and that work established the idea of a very small type-II band offset. We will now briefly describe the problem and the method employed in Ref. 3.

Figure 1(a) gives a schematic overview of the band alignment in a Si/$Si_{1-x}Ge_x$/Si single quantum well (SQW) with no external stress applied. In Si the conduction-band (CB) edge is formed by six degenerate valleys at the Δ minima of the Brillouin zone and the valence-band (VB) edge is formed by degenerate heavy-hole (hh) and light-hole (lh) bands at the Γ point. $Si_{1-x}Ge_x$ exhibits a Si-like band structure for $x<0.85$, but as the relaxed lattice parameter of $Si_{1-x}Ge_x$ is larger than that of Si, there is an internal biaxial compressive stress acting on the $Si_{1-x}Ge_x$ epilayers grown on Si(001) substrates. This stress partially lifts the degeneracy of the six Δ valleys, the four valleys in the QW plane (Δ_4 from now on) are lowered, and the two valleys in the [001] growth direction (Δ_2) are raised. Figure 1(b) represents a Fermi surface for the Si conduction band and illustrates the definition of Δ_4 and Δ_2 valleys. The stress also lifts the hh-lh degeneracy, the hh band is raised, and the lh lowered. For a QW with $x=0.3$ the hh offset and the splitting between Δ_2 and Δ_4 band are both on the order of 200 meV (see Appendix). Therefore the holes are well confined to the $Si_{1-x}Ge_x$ layer and the Δ_2 conduction band in the $Si_{1-x}Ge_x$ is clearly above the Si conduction band. The controversial point about the band structure is whether the Δ_4 band in the $Si_{1-x}Ge_x$ lies above or below the Si conduction band, which leads to a type-II or type-I band alignment, respectively [in Fig. 1(a) a type-II case is shown, i.e., $U_e(\Delta_4)>0$]. In contrast to, e.g., Ref. 3 we will use the terms ''type-II'' and ''type-I'' strictly equivalent to the sign of the Δ_4 CB offset.

The effect of low uniaxial [110] stress on the bands has

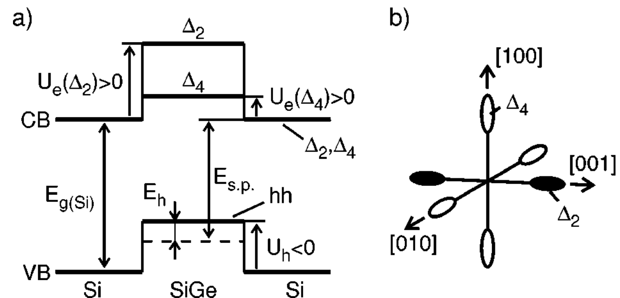

FIG. 1. (a) Schematic overview of the band alignment in a $Si_{1-x}Ge_x$ QW. The conduction band (CB) is six-fold degenerate in the Si and split into Δ_4 and Δ_2 valleys in the $Si_{1-x}Ge_x$. A heavy-hole- (hh) like band forms the QW for the holes. Energies defined in the text are illustrated. (b) Schematic picture of a Fermi surface in the Si CB defining Δ_4 (open ellipsoids) and Δ_2 (filled ellipsoids) valleys.

0163-1829/99/59(20)/13314(8)/$15.00 PRB 59 ©1999 The American Physical Society

been treated in Ref. 2. For Δ_4 electrons the CB is raised in energy at almost the same rate in the Si and $Si_{1-x}Ge_x$ layers (about 14 meV/GPa), whereas for Δ_2 electrons the CB is lowered throughout the structure at approximately twice the rate. The hh VB in the $Si_{1-x}Ge_x$ is lowered in energy at a smaller rate (11.2 meV/GPa). The numbers differ for (001) biaxial stress, but the qualitative behavior is the same.

The idea behind the stress experiments is that for a type-II band alignment the Si layers should be energetically favorable for electrons. Therefore the electron energy should be lowered with the high rate for Δ_2 electrons, and since the lowering of the hh band in $Si_{1-x}Ge_x$ occurs with a lower rate, the energy observed in photoluminescence (PL) should decrease. For the type-I case the electrons should favor the $Si_{1-x}Ge_x$ layer, and therefore go up in energy with the rate for Δ_4 electrons. Together with the lowering of the hh band this should add up to an increase of the photon energy observed in PL. The conclusion was that the sign of the energy shift due to the application of tensile [110] or (001) stress directly decides the type-II vs type-I question.[2]

There is a serious problem with this interpretation, namely, that it reduces the recombination process to calculating the energy difference between the overall CB minimum and the overall VB maximum. This neglects the fact that the PL originates from the recombination of excitons and not from recombination of free electrons and holes. Since the hole is confined to the $Si_{1-x}Ge_x$ layer and the electron is bound to the hole, it is clear that the exciton energy will be influenced by the conduction-band energy in the $Si_{1-x}Ge_x$ layer. In particular, without external stress and neglecting the different effective masses of Δ_2 and Δ_4 electrons, Δ_4-hh excitons would always be energetically favorable, since in that case the Δ_2 conduction band is degenerate with the Δ_4 band in the Si layers and far above the Δ_4 band in the $Si_{1-x}Ge_x$ layer. From this simple consideration it could therefore be concluded that the application of tensile [110] or (001) stress will always lead to an initial blueshift of the PL, regardless of the CB offset, since the lowest exciton state is always a Δ_4 state and the applied stress leads to an upshift in energy of the whole Δ_4 conduction band.

Houghton *et al.*[2] observed only Δ_4 recombination in their experiments and concluded from consideration of the overall CB minima that this implies a type-I offset of at least 10 meV for $x=0.15$. But the more recent paper of Thewalt *et al.*[3] revealed that excitation power can alter the behavior observed in the stress experiments. The authors demonstrated on a 3 nm wide $Si_{0.7}Ge_{0.3}$ QW that with decreasing excitation power a Δ_4 to Δ_2 transition can be observed at smaller and smaller tensile stress values and they finally found that at the lowest power Δ_2 behavior is observed even without external stress. From this they concluded a type-II alignment, following the argumentation of Houghton *et al.*,[2] with the offset being ''small.'' As they also referred to the 10 meV Houghton *et al.*[2] had claimed earlier as ''surprisingly large'' this led to the assumption that a type-II offset of less than 10 meV was in fact proven[4] or even to the claim that a 1 meV type-II CB offset was shown.[5] The latter work also involved PL measurements under stress and proposed type-II CB offsets on the order of 5 meV for $x=0.3$ and 0.5, because there they also saw Δ_2 behavior in the limit of low stress.

As pointed out earlier, Δ_2 behavior without external stress can *a priori* not be understood at all. Especially with the small offsets under consideration Δ_4 excitons should be the energetically favorable ones, since the electrons can gain the $Si_{1-x}Ge_x$ exciton binding energy, which is on the order of 15 meV, by overcoming the comparably small energy barrier. It is therefore highly desirable to achieve a less simplified view of the recombination in such structures. This paper intends to improve the understanding of excitons in $Si_{1-x}Ge_x$ quantum wells by calculating exciton ground-state wave functions and energies for Δ_4-hh and Δ_2-hh excitons, oscillator strengths, and binding energies in dependence on the Δ_4 CB offset and for different well widths.

II. THEORETICAL MODEL

We will apply an effective mass model allowing for different in-plane and perpendicular masses of the electron and hole to obtain two-particle wave functions for excitons in a quantum well. In this model the Schrödinger equation can be written as[6]

$$\left[-\frac{\hbar^2}{2m_\rho}\frac{1}{\rho}\frac{\partial}{\partial\rho}\rho\frac{\partial}{\partial\rho}-\frac{\hbar^2}{2m_{ez}}\frac{\partial^2}{\partial z_e^2}+U_e(z_e)-\frac{\hbar^2}{2m_{hz}}\frac{\partial^2}{\partial z_h^2}+U_h(z_h)-\frac{e^2}{4\pi\varepsilon_0\varepsilon}\frac{1}{\sqrt{\rho^2+(z_e-z_h)^2}}\right]\psi(\rho,z_e,z_h)=E\psi(\rho,z_e,z_h), \tag{1}$$

where

$$\frac{1}{m_\rho}=\frac{1}{m_{e\rho}}+\frac{1}{m_{h\rho}}$$

and

$$U_{e,h}(z)=\begin{cases}0 & \text{for } |z|\geq L/2\\ U_{e,h} & \text{for } |z|<L/2.\end{cases}$$

The z axis is chosen as the [001] growth direction, with $z=0$ in the center of the QW. The xy plane is therefore the plane of the QW. The in-plane and perpendicular electron (hole) masses are denoted as $m_{e(h)\rho}$ and $m_{e(h)z}$, respectively; m_ρ is the reduced in-plane mass. The conduction- (valence-) band offset is named $U_{e(h)}$, with negative values indicating that the QW is favorable for the electron (hole). L is the quantum well width, $z_{e(h)}$ the z coordinate of the electron (hole), ρ is the in-plane electron-hole distance, and E is the eigenenergy of the eigenstate ψ. The permittivity of free space and the dielectric constant are denoted as ε_0 and ε, respectively.

To obtain Eq. (1), center of mass and relative coordinates in the xy plane have to be used, with the relative coordinates being introduced in polar notation (ρ,φ). Solutions depending on the center of mass coordinates correspond to states with nonzero total momentum in the xy plane, and solutions depending on the polar angle φ correspond to states with nonzero angular momentum in z direction. As we want to explain PL measurements, we are only interested in the absolute ground state and can therefore restrict the calculations to functions $\psi(\rho,z_e,z_h)$.

The numerical method to solve Eq. (1) for the ground state and details of the calculations and the material parameters we used are given in the Appendix. Main simplifications of the approach are the restriction to in-plane and perpendicular masses and the assumption of material independence of the masses and the dielectric constant. These simplifications are necessary to keep our numerical method feasible, nevertheless they should not lead to serious errors. For the electron masses no significant difference between Si and $Si_{1-x}Ge_x$ is expected,[7] and the dielectric constant ε changes just by 10% from Si to $Si_{0.7}Ge_{0.3}$, which makes an averaged value a good approximation. The situation is more complicated for the holes, but they are strongly confined to the $Si_{1-x}Ge_x$ layer and therefore the values for $Si_{1-x}Ge_x$ are appropriate. Also one should keep in mind that we are mainly interested in the distribution of the electrons. Our approach yields two-particle wave functions, describing the ground state of a single exciton. It should be well suited for describing the very situation of extremely low excitation powers, as investigated, e.g., by Thewalt *et al.*,[3] but it does in principle not include many particle features, in particular, electric fields generated from additional excitons.

In the next section we will use the following functions, which are derived from ψ, to discuss numerical results:

$$p(z_e,z_h)=2\pi\int_0^\infty d\rho\rho|\psi(\rho,z_e,z_h)|^2,$$

$$p_{e,h}(z_{e,h})=2\pi\int_0^\infty d\rho\rho\int_{-\infty}^\infty dz_{h,e}|\psi(\rho,z_e,z_h)|^2,$$

$$\zeta(z)=|\psi(0,z,z)|^2,$$

$$|f|^2=\left|\int_{-\infty}^\infty dz\,\psi(0,z,z)\right|^2.$$

The function $p(z_e,z_h)$ gives the probability density to find the electron at z_e and the hole at z_h, regardless of ρ. The function $p_{e(h)}(z_{e(h)})$ gives the probability density to find the electron (hole) at $z_{e(h)}$, regardless of ρ and $z_{h(e)}$. A kind of overlap function is represented by $\zeta(z)$, which is proportional to the probability to find the electron and the hole at the same place. It can be used to estimate where in the structure recombination takes place. The oscillator strength $|f|^2$ will be employed to discuss recombination probabilities, although it should be mentioned that these two quantities are not exactly proportional in indirect semiconductors.

From the definition of $U_{e,h}$ it follows that E gives the recombination energy of the exciton relative to the Si band gap ($E_{g(\mathrm{Si})}$, 1.17 eV). We will also use the quantities $E_X=E+E_{g(\mathrm{Si})}$, which gives the absolute exciton recombination energy, and $E_b=E_{\mathrm{SP}}-E_X$, the exciton binding energy. E_{SP} is the recombination energy which is obtained in a single-particle picture, where the Coulomb interaction is not taken into account. With $U_h<0$, it is given by

$$E_{\mathrm{SP}}=\begin{cases}E_{g(\mathrm{Si})}+U_h+E_h+U_e+E_e & \text{for } U_e<0\\ E_{g(\mathrm{Si})}+U_h+E_h & \text{for } U_e\geqslant 0,\end{cases} \quad (2)$$

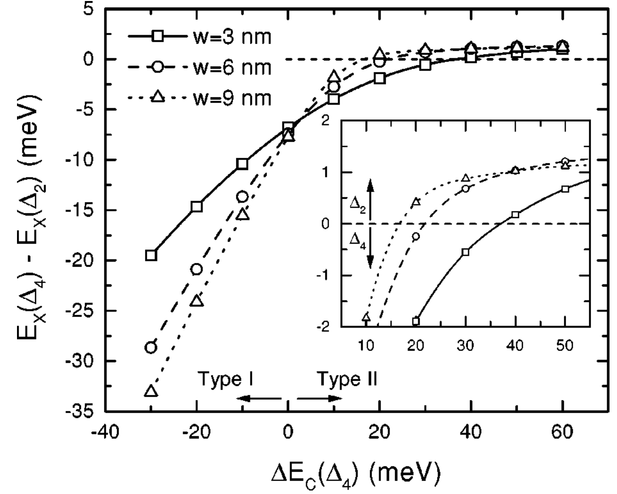

FIG. 2. The difference in recombination energy between Δ_4- and Δ_2-hh excitons, as a function of the band offset in the Δ_4 conduction band [$\Delta E_C(\Delta_4)$, or $U_e(\Delta_4)$]. A positive value means that the Δ_2 exciton is favorable, a negative value that the Δ_4 exciton is favorable. The inset is a zoom to the range where the value changes sign. The excitons differ in the electron masses and in the conduction-band offset [$U_e(\Delta_2)=U_e(\Delta_4)+202.6$ meV]. The calculations refer to $Si_{0.7}Ge_{0.3}$ QWs with well widths of 3, 6, and 9 nm. The lines connecting data points are guides to the eye.

where E_e and E_h are single-particle confinement energies. Figure 1(a) illustrates the definitions of the energies $E_{g(\mathrm{Si})}$, E_h, E_{SP}, U_e, and U_h for a type-II situation.

III. RESULTS AND DISCUSSION

We will first consider $E_X(\Delta_4)-E_X(\Delta_2)$, the energy difference between the Δ_4-hh and the Δ_2-hh exciton in the same structure. A positive value means that the Δ_2-hh exciton is the ground state, a negative value that the Δ_4-hh exciton is energetically favorable. The two types of excitons differ by the electron masses ($m_{e\rho}$ and m_{ez}) and by the conduction-band offset. For $x=0.3$ it is valid that $U_e(\Delta_2)\approx U_e(\Delta_4)+200$ meV.

Figure 2 shows the variation of the energy difference with the Δ_4-CB offset $\Delta E_C(\Delta_4)=U_e(\Delta_4)$ for 3, 6, and 9 nm wide $Si_{0.7}Ge_{0.3}$ quantum wells. It should be mentioned that $E_X(\Delta_2)$ hardly changes with $U_e(\Delta_4)$ [see also $E_b(\Delta_2)$ in Fig. 9]. In this figure the barrier for the Δ_2 electrons, $U_e(\Delta_2)$, varies just between 170 and 260 meV. Because of the high perpendicular electron mass for these excitons [$m_{ez}(\Delta_2)=0.92m_0$], this acts as an almost infinite barrier throughout. Therefore the variation in Fig. 2 only originates from variations in $E_X(\Delta_4)$.

On the type-I side it can be seen that $E_X(\Delta_4)$ drops faster for wider wells, which can be understood in a single-particle picture, because here the quantized electron level follows an increasing depth of the QW more directly. For flatband ($\Delta E_C=0$) and small type-II offsets the Δ_4-hh exciton stays energetically favorable, which is consistent with the considerations in the Introduction. It also proves that PL measurements under applied stress are not unambiguous, because in this range an initial blueshift with increasing tensile stress would be observed, in spite of the type-II band alignment.

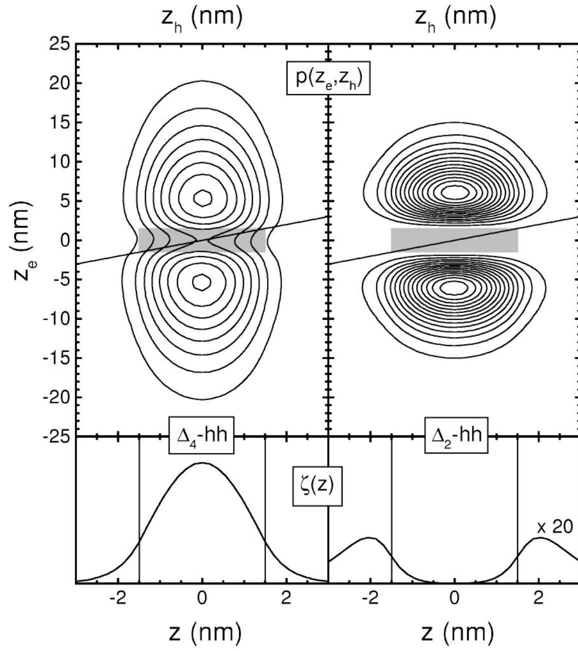

FIG. 3. Contour plots of the functions $p(z_e,z_h)$ (top) and plots of the functions $\zeta(z)$ (bottom) for a Δ_4-hh exciton (left) and a Δ_2-hh exciton (right). The calculations refer to a 3 nm wide $Si_{0.7}Ge_{0.3}$ QW and a type-II conduction-band offset $U_e(\Delta_4)=40$ meV. The vertical lines in the bottom indicate the QW borders and the gray areas in the top indicate the region where electron and hole reside in the QW. The tilted lines in the top mark the condition $z_e=z_h$. Although $\zeta(z)$ is given in arbitrary units, it can be compared between left and right side (note the enhancement factor of 20 for the right side). The lines of the contour plots are at identical values for both sides.

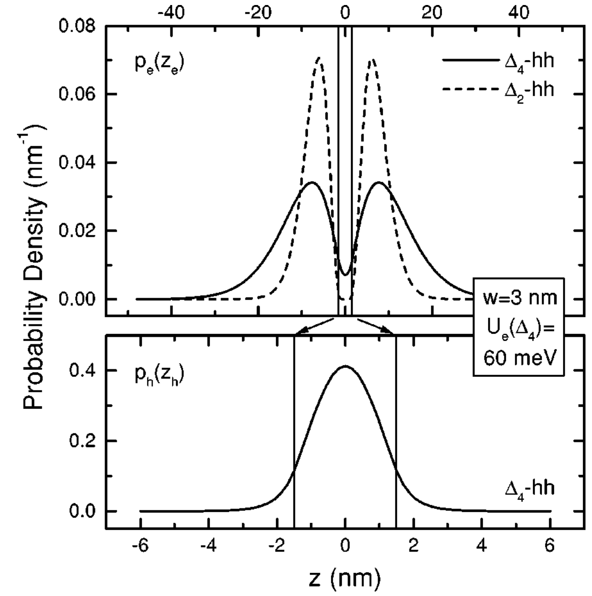

FIG. 4. Plot of the functions $p_e(z_e)$ for the Δ_2- and Δ_4-hh exciton (top) and $p_h(z_h)$ for the Δ_4-hh exciton (bottom) in a 3 nm wide $Si_{0.7}Ge_{0.3}$ QW with a type-II conduction-band offset $U_e(\Delta_4)=60$ meV. $p_{e(h)}(z_{e(h)})$ gives the probability for the electron (hole) to be at a certain z coordinate. The vertical lines indicate the QW borders.

But the most interesting observation in Fig. 2 is that indeed the Δ_4-hh exciton can be energetically above the Δ_2-hh exciton, although only at rather high type-II offsets in the Δ_4 conduction band. The changeover from Δ_4- to Δ_2-like behavior takes place at offsets of about $U_e(\Delta_4)=37$, 22, and 17 meV for well widths of 3, 6, and 9 nm, respectively.

From Eq. (2) it follows that E_{SP} is independent of any conduction-band property as long as $U_e(\Delta_4)>0$. Since $E_X=E_{SP}-E_b$, this means that in the type-II range $E_X(\Delta_4)-E_X(\Delta_2)$ is identical to $E_b(\Delta_2)-E_b(\Delta_4)$. The question of why the Δ_2-hh exciton can be energetically favorable is therefore identical to the question of why the binding energy of the Δ_2-hh exciton can become larger than the binding energy of the Δ_4-hh exciton.

We will now concentrate on a width of 3 nm, which corresponds to the sample investigated in Ref. 3. An explanation for the changeover can be given from looking at the functions $p(z_e,z_h)$ for the two types of excitons. Contour plots of these functions are shown in the upper part of Fig. 3 for $U_e(\Delta_4)=40$ meV (i.e., close to the changeover). On the one hand it can be seen that the electrons have a higher probability to be in the QW for the Δ_4-hh exciton, which should result in an increased binding energy. But on the other hand it is also clear that the electron distribution leaks farther into the Si layer for the Δ_4-hh exciton. This is because of the smaller perpendicular electron mass for the Δ_4 CB ($0.19m_0$, compared to $0.92m_0$ for the Δ_2 CB), and should result in a decreased binding energy. At high type-II CB offset the second effect can dominate and make the Δ_2-hh exciton favorable. The inclined lines mark $z_e=z_h$ and are intended to assist in this consideration, as the distribution should stay close to this line in order to achieve high binding energies.

The bottom part of Fig. 3 gives the functions $\zeta(z)$ for the two exciton types. It is interesting that at this large type-II Δ_4-CB offset the overlap function for the Δ_4-hh exciton has its maximum still clearly in the QW, although the electron distribution is already pushed considerably into the Si layers. Only for the Δ_2-hh exciton are the overlap maxima also pushed into the Si layers, and of course the overlap is very small. This explains the long lifetime of Δ_2-hh excitons and the missing Ge-related phonon replicas in Δ_2 PL spectra.[3] It also shows that the presence of these replicas in Δ_4 spectra implies neither any band bending effects nor a small CB offset (even at $U_e=60$ meV the Δ_4 overlap maximum is still in the QW).

In the top of Fig. 4 the electron distribution functions $p_e(z_e)$ are plotted for both types of excitons for $U_e(\Delta_4)=60$ meV. Again it can be seen that the Δ_4 electrons have a higher probability to be in the $Si_{1-x}Ge_x$ layer, but also penetrate further into the Si layers than the Δ_2 electrons. The bottom part of Fig. 4 shows the corresponding function $p_h(z_h)$ for the heavy hole bound to the Δ_4 electron. As already claimed in Sec. II, the holes are well confined to the $Si_{1-x}Ge_x$ layer, even in this thin well. It should be mentioned that the function $p_e(z_e)$ for the Δ_2-hh exciton does not change much with $U_e(\Delta_4)$, and also that $p_h(z_h)$ is virtually identical for all types of electrons and values of $U_e(\Delta_4)$. What changes drastically with $U_e(\Delta_4)$ is $p_e(z_e)$ for the Δ_4-hh exciton, as can be seen in Fig. 5. Note that at an offset of $U_e=10$ meV the maximum of $p_e(z_e)$ is still in the QW, and only at $U_e\geqslant 20$ meV is a dip observable. As could

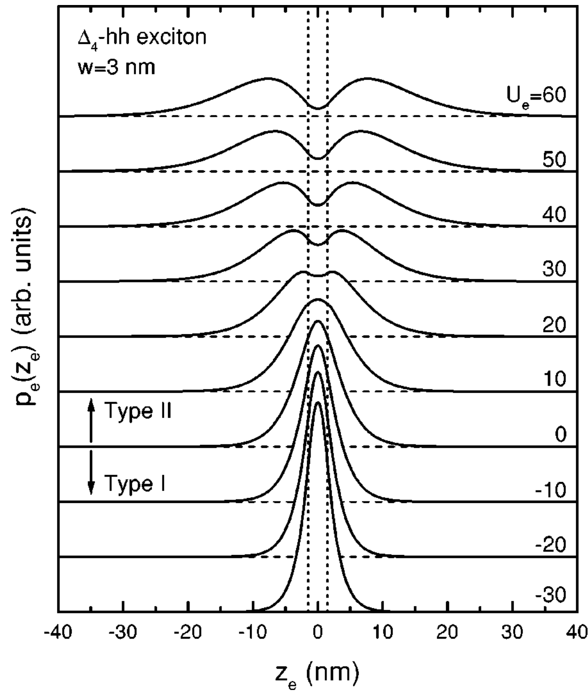

FIG. 5. Plot of the functions $p_e(z_e)$ for the Δ_4-hh exciton in a 3 nm wide $Si_{0.7}Ge_{0.3}$ QW for different conduction-band offsets $U_e(\Delta_4)$. The function $p_e(z_e)$ gives the probability for the electron to be at a certain z coordinate. The vertical dotted lines indicate the QW borders.

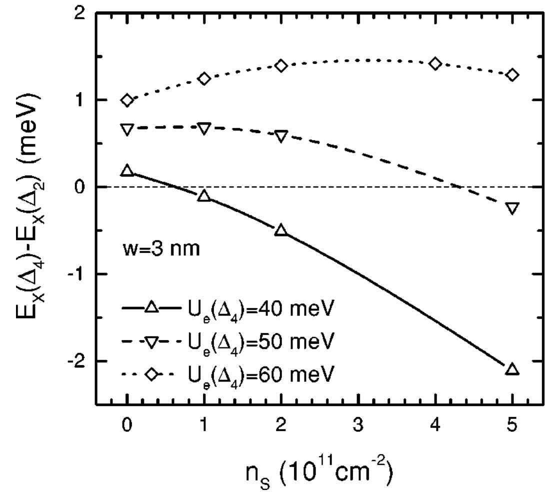

FIG. 6. The difference in recombination energy between Δ_4- and Δ_2-hh excitons for a 3 nm wide $Si_{0.7}Ge_{0.3}$ QW, as a function of band bending (characterized by a sheet carrier concentration n_S). A positive value means that the Δ_2 exciton is favorable, a negative value that the Δ_4 exciton is favorable. The lines connecting data points are guides to the eye.

be expected, only offsets which are higher than the bulk exciton binding energy lead to a considerable displacement of the electrons.

We already mentioned that the calculations for a well width of 3 nm presented in Fig. 2 correspond to the sample investigated in Ref. 3. This leads to the conclusion that the observation of Δ_2 behavior in the absence of external stress reported in Ref. 3 is only consistent with a type-II CB offset of about 40 meV or more. Of course there is a remarkable discrepancy to the value of 1 meV given in Ref. 5, which was obtained from the observation that already extremely low excitation powers are sufficient for a changeover to Δ_4 behavior. Rowell *et al.*[5] considered what value for the energy barrier height can be overcome by band bending at such low excitation powers. Taking into account that the barrier which has to be overcome is not the CB offset but the energy difference between Δ_2- and Δ_4-exciton states, the discrepancy could be explained, since this energy difference is indeed on the order of 1 meV, even for the highest calculated offset $U_e = 60\,\text{meV}$. Although our model treats single excitons, we will try to account qualitatively for band bending effects by including an electrostatic potential $\Phi(z)$. We construct this potential from a charge distribution $\rho(z)$, which is given as

$$\rho(z) = e n_S [p_h(z) - p_e(z)].$$

Here e is the electron charge, n_S plays the role of a sheet density of carriers, and p_h and p_e are taken from the wave function for the Δ_2-hh exciton [resulting at $\Phi(z) \equiv 0$]. The potential $\Phi(z)$ follows from the Poisson equation

$$\frac{\partial^2}{\partial z^2}\Phi(z) = -\frac{\rho(z)}{\varepsilon_0 \varepsilon}$$

by numerically integrating over ρ twice. It can then be included into the calculation by adding $[e\Phi(z_h) - e\Phi(z_e)]\,\psi$ to the left side of Eq. (1); no other modifications are required. Resulting Δ_2-hh wave functions are not used to calculate a new function $\rho(z)$ since the intention is only to check for the influence of band bending, this is no real many-particle solution anyway.

Figure 6 shows how the energy difference $E_X(\Delta_4) - E_X(\Delta_2)$ varies with band bending (characterized by the parameter n_S) for the 3 nm wide QW and CB offsets of $U_e(\Delta_4) = 40$, 50, and 60 meV. At $n_S = 0$ the value is positive for all offsets, which means that the Δ_2-hh exciton is favorable. At an offset of 40 meV, which is very close to the changeover from Δ_2 to Δ_4 behavior, at $n_S = 1\times10^{11}\,\text{cm}^{-2}$ the transition to Δ_4 behavior has already occurred. The band bending pushes the Δ_4 electrons further into the $Si_{1-x}Ge_x$ barrier and therefore increases the binding energy of the Δ_4-hh exciton. But at an offset of 50 meV the transition occurs at much higher densities, probably at about $n_S = 4.3 \times 10^{11}\,\text{cm}^{-2}$, and at an offset of 60 meV it has not occurred even at $n_S = 5\times10^{11}\,\text{cm}^{-2}$. For these higher offsets another effect is important, namely, that the confinement mass for the Δ_2 electrons in z direction is higher. Therefore their single-particle energy would not be raised as much due to an overall band bending as the corresponding energy of the Δ_4 electrons. The counteracting effect that the binding energy of the Δ_4-hh exciton increases is still present, but with increasing offset it takes higher values of n_S to make this effect dominant.

From Fig. 6 it follows that bend bending can cause a changeover from a Δ_2 ground state to a Δ_4 ground state, and that this mechanism is only efficient when the CB offset is rather close to the offset where the Δ_2/Δ_4 changeover would take place anyway. But the energy difference between the

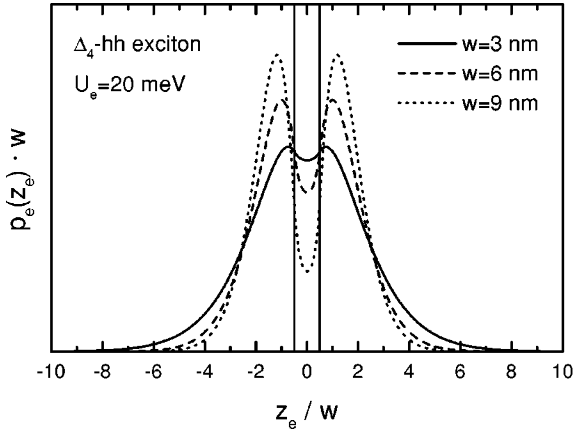

FIG. 7. Rescaled electron distributions $p_e(z_e)w$ as a function of z_e/w for Δ_4-hh excitons in QWs with widths of 3, 6, and 9 nm and a type-II CB offset $U_e(\Delta_4)=20$ meV. Because of the rescaling of the z axis the QW boundaries (vertical lines) coincide for all well widths, and the rescaling of the electron distribution serves to keep the area under the graphs constant.

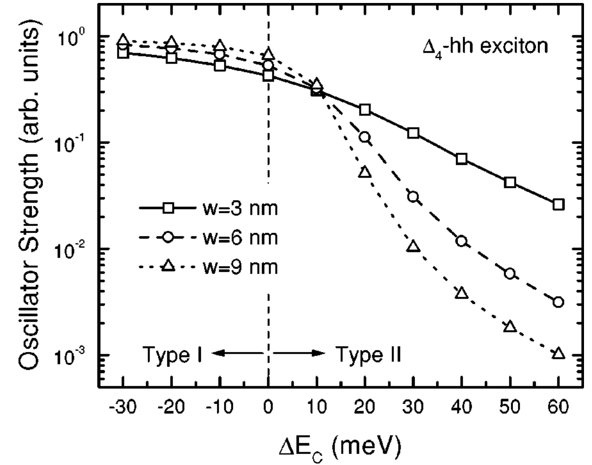

FIG. 8. The oscillator strength $|f|^2$ for Δ_4-hh excitons as a function of the band offset in the Δ_4 conduction band $[\Delta E_C$ or $U_e(\Delta_4)]$. The calculations refer to $Si_{0.7}Ge_{0.3}$ QWs with well widths of 3, 6, and 9 nm. The lines connecting data points are guides to the eye. The dashed vertical line gives the separation between type-II and type-I offsets.

two types of excitons is always very small when the Δ_2-hh exciton forms the ground state, and the Δ_4-hh exciton will always have a much higher oscillator strength. Therefore one should be aware that in a PL experiment Δ_4 luminescence can dominate even when the Δ_2-hh exciton forms the ground state, because of either the Fermi energy lying above the Δ_4 level or because of thermal occupation of this higher level.

In Fig. 7 the rescaled electron distributions $p_e(z_e)$ w are given as a function of z_e/w for Δ_4-hh excitons, well widths of 3, 6, and 9 nm, and $U_e=20$ meV. Because of the rescaling of the z axis the QW boundaries coincide for all well widths, and the rescaling of the electron distribution serves to keep the area under the graphs constant. This figure is intended to facilitate the comparison between different well widths, mainly with respect to the probability that the electron is found in the QW. For comparing the extension of the distributions it has to be taken into account that their z scales are different. Figure 7 shows that at higher QW widths Δ_4 electrons are more efficiently displaced by a type-II CB offset. The probability to find the electrons outside of the $Si_{1-x}Ge_x$ layer increases. Since the mechanism which favors Δ_2 recombination requires a high extension of the Δ_4-electron distribution into the Si layers, Fig. 7 yields an explanation for the fact that the type-II offset which is needed to make the Δ_2-hh exciton energetically favorable decreases with increasing well width (see Fig. 2). From this point of view narrow wells seem not to be the most suited ones for the observation of Δ_2-like behavior.

In Ref. 3 the Δ_2/Δ_4 transition already at very low excitation powers was interpreted as a ''type-II''/''type-I'' transition, and it was claimed that the PL observed in all of the previously published literature was ''type-I'' because excitation-power-induced band bending would have moved the electrons into the $Si_{1-x}Ge_x$ layer. This suggested that information on the intrinsic CB offset can only be obtained at extremely low excitation powers. In fact that work has shown that Δ_2-like recombination can only be seen at extremely low excitation powers and that all previously observed PL was Δ_4-like. Therefore it still makes sense to do PL measurements at more usual excitation powers; one could even be of the opinion that this would be preferable, since only the properties of the Δ_4-hh excitons depend significantly on the Δ_4 CB offset, which is the quantity under question. In the following we will try to relate some results of our calculations to observations from such PL measurements.

Figure 8 shows the oscillator strength $|f|^2$ for Δ_4-hh excitons in dependence on the CB offset for different well widths. Of course the oscillator strength increases with decreasing U_e (i.e., going from type-II to type-I offsets). If the type-II offset is larger than 10 meV, the oscillator strength decreases strongly with well width, which is due to the increasing separation of the electron and the hole. For $U_e \leqslant 0$ it increases slightly with well width. This can be understood when one considers that the hole distribution is always well confined to the QW, whereas the electron distribution will leak into the Si layers considerably when the type-I offset is small and the QW is narrow [compare $p_h(z_h)$ in Fig. 4 and $p_e(z_e)$ in Fig. 5]. Therefore, in a wider well the electron distribution will better match with the hole distribution, leading to an increased oscillator strength. Although to our knowledge not explicitly published, it has been observed by several groups that narrow $Si_{1-x}Ge_x$ quantum wells tend to exhibit stronger luminescence than wider ones. According to our calculation this behavior can be explained solely from considering the oscillator strength, as long as the CB alignment is type II with an offset of more than 10 meV.

Figure 9 finally shows how the exciton binding energy of the Δ_4-hh exciton varies with CB offset and well width. These results can be compared with the variational calculations performed by Baier *et al.*,[8] and although our approach yields slightly higher binding energies, the qualitative behavior is the same. At flatband or type-I conditions the binding energy is not highly dependent on well width, but already with a small type-II CB offset it decreases strongly with well width. An experimentally accessible quantity that depends on the binding energy is the diamagnetic shift in PL experiments in magnetic field, which increases with decreasing

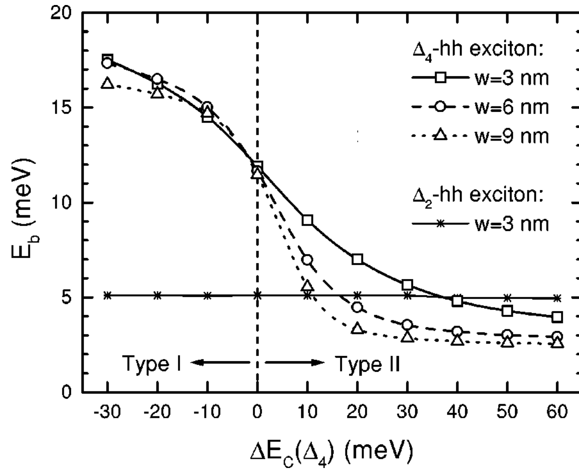

FIG. 9. The binding energy of Δ_4- and Δ_2-hh exciton as a function of the band offset in the Δ_4 conduction band $[\Delta E_C(\Delta_4)$ or $U_e(\Delta_4)]$. The calculations refer to $Si_{0.7}Ge_{0.3}$ QWs with well widths of 3, 6, and 9 nm. The lines connecting data points are guides to the eye. The dashed vertical line gives the separation between type-II and type-I offsets.

binding energy. Magneto-optical investigations on a series of $Si_{0.76}Ge_{0.24}$ QWs with different well widths[9] have indeed shown that the diamagnetic shift increases strongly with well width, and therefore again yielded strong support for a type-II band alignment. The binding energy of the Δ_2-hh exciton for a well width of 3 nm is also included in Fig. 9. As stated earlier, it can be seen that the energy of this exciton is almost constant over the investigated range of Δ_4 CB offsets. This is also true for the well widths of 6 and 9 nm.

IV. CONCLUSION

The observation of energy shifts due to the application of small tensile stress in PL measurements on $Si/Si_{1-x}Ge_x$ quantum wells yields information on whether the electrons involved occupy Δ_2 or Δ_4 minima of the conduction band. We pointed out that only Δ_4-like behavior can be explained from simple considerations. Anyhow, Δ_2-like behavior was reported in recent PL experiments at extremely low excitation powers on a 3 nm wide $Si/Si_{0.7}Ge_{0.3}$ QW.[3] We therefore performed numerical calculations of the two-particle ground-state wave functions and energies both for Δ_4-hh and Δ_2-hh excitons in $Si/Si_{0.7}Ge_{0.3}$ quantum wells. These calculations show that Δ_2 behavior can occur because of the different effective electron masses for the Δ_2 and the Δ_4 conduction band. The observations in Ref. 3 can therefore be explained, but only with a type-II offset for the Δ_4 conduction band of about 40 meV, which is a much larger offset than was considered so far.

Our calculations also yield overlap functions for the different excitons, and we showed that the Δ_2-hh overlap function is pushed out of the QW considerably, which explains the absence of Ge-related phonon replicas in Δ_2-like PL signals. On the other hand, even for large type-II offsets the Δ_4-hh overlap function has its maximum inside the QW, therefore Ge-related phonon replicas are expected.

We showed for Δ_4-hh excitons how the electron distribution varies with the CB offset, and in particular that only type-II offsets of more than 10 meV can push the electrons out of the QW considerably. The inclusion of band bending in the calculations yielded a possible mechanism for the excitation-power-induced change from Δ_2-like to Δ_4-like PL, but we also pointed out that, as long as the Δ_2 exciton forms the ground state, the energy differences between the two types of excitons are so small that filling effects could play a role. We demonstrated how oscillator strength and binding energy of the Δ_4-hh exciton vary with CB offset and well width and found that experimental observations of these quantities also support a type-II band alignment.

TABLE I. Selected properties of Si and Ge, which are used to obtain values for $Si_{1-x}Ge_x$ by linear interpolation.

	Si	Ge	Comment
ε	12.1	16.0	Ref. 13
a (Å)	5.4296	5.6567	
c_{11} (Mbar)	1.675	1.315	Ref. 14
c_{12} (Mbar)	0.650	0.494	Ref. 14
Ξ_u^Δ (eV)	9.16	9.42	Ref. 11

ACKNOWLEDGMENTS

We want to acknowledge financial support by the Österreichische Nationalbank (ÖNB), the Gesellschaft für Mikroelektronik (GMe), the Fonds zur Förderung der wissenschaftlichen Forschung (FWF), and the Bundesministerium für Wissenschaft und Verkehr.

APPENDIX: MATERIAL PARAMETERS AND NUMERICAL METHOD

To obtain an estimate of the valence-band offset in $Si_{1-x}Ge_x$ we used the band-gap formula given in Ref. 10 and the assumption that the whole change is due to the valence band. This gives a valence-band offset $\Delta E_{VB}=227.9$ meV for $x=0.3$. For the conduction-band splitting we used the formula[11]

$$E_{CB}(\Delta_2)-E_{CB}(\Delta_4)=\Xi_u^\Delta\left(\frac{a_{Si}}{a}-1\right)\left(-2\frac{c_{12}}{c_{11}}-1\right),$$

where the quantities on the right-hand side can be obtained by linear interpolation between the Si and Ge values given in Table I. This leads to a splitting of 202.6 meV for $x=0.3$. For the dielectric constant we used the linearly interpolated value for $x=0.15$, i.e., the averaged value over the Si and the $Si_{0.7}Ge_{0.3}$ value, which yields $\varepsilon=12.7$. We calculated the Luttinger parameters following Ref. 7 to be $\gamma_1=4.79$ and $\gamma_2=0.55$ at $x=0.3$ and the heavy-hole masses in the decoupled limit $m_{h\rho}=m_0/(\gamma_1+\gamma_2)$ and $m_{hz}=m_0/(\gamma_1-2\gamma_2)$, which yields $0.19m_0$ and $0.27m_0$, respectively. From Ref. 7 it can also be seen that for the electron masses it is sufficient to use Si values throughout. In Table II the masses which result for Δ_2 and Δ_4 electrons are given, where the in-plane electron mass $m_{e\rho}$ is calculated as a two-dimensional density of states mass ($\sqrt{m_{ex}m_{ey}}$).

The method we used for solving Eq. (1) for the ground state is described in Ref. 12. It can be interpreted as the

TABLE II. In-plane ($m_{e\rho}$) and perpendicular (m_{ez}) electron masses for Δ_2 and Δ_4 electrons.

	Δ_2	Δ_4
$m_{e\rho}=\sqrt{m_{ex}m_{ey}}$	$0.19m_0$	$0.42m_0$
m_{ez}	$0.92m_0$	$0.19m_0$

evolution of a wave function into imaginary time. The time-dependent Schrödinger equation and its solutions can be written as

$$i\hbar\frac{\partial}{\partial t}\psi(R,t)=H\psi(R,t), \tag{A1}$$

$$\psi(R,t)=\sum_{n=0}^{\infty}c_n\varphi_n(R)e^{-iE_nt/\hbar}, \tag{A2}$$

where H is the Hamilton operator, t is the time, R represents all coordinates but time, and φ_n and E_n are the eigenstates and eigenenergies (with $E_{n+1}\geqslant E_n$) of the corresponding time-independent equation. Introducing $\tau=it/\hbar$ and $\Psi(R,\tau)=\psi(R,\hbar\tau/i)=\psi(R,t)$, Eqs. (A1) and (A2) become

$$-\frac{\partial}{\partial\tau}\Psi(R,\tau)=H\Psi(R,\tau), \tag{A3}$$

$$\Psi(R,\tau)=\sum_{n=0}^{\infty}c_n\varphi_n(R)e^{-E_n\tau}. \tag{A4}$$

From Eq. (A4) it can be seen that Ψ will be increasingly dominated by φ_0 for increasing τ, as E_0 is the smallest energy appearing in the exponential terms. Reference 12 describes how to discretize Eq. (A3) and how the convergence of the method towards the ground-state $\varphi_0(R)$ can be accelerated.

The space domain which was used for the calculations in this paper is given by

$$(\rho,z_e,z_h)\in[0,16w]\times[-16w,16w]\times[0,2w],$$

where w is the QW width. z_h can be restricted to positive values, because from the symmetry of the Hamiltonian in Eq. (1) it follows that the ground state fulfills

$$\psi(\rho,z_e,-z_h)=\psi(\rho,-z_e,z_h).$$

We used vanishing boundary conditions (not at the boundaries $\rho=0$ and $z_h=0$, of course), and the grid spacing $\Delta\rho$ and Δz were chosen as $w/8$ and $w/16$, respectively. To make sure that the boundaries are not too close we tentatively doubled the extension of the domain and the corresponding number of points in certain coordinates for critical conditions, and to make sure that the grid is dense enough we tentatively doubled the number of points while leaving the extension unchanged. Typically this led to changes in the ground-state energy of at most 0.15 meV, only the error for the Δ_2-hh exciton in the $w=9$ nm well is a bit larger (0.26 meV).

[1] V. P. Kesan, S. Shubbana, P. J. Restle, M. J. Tejwani, J. M. Aitken, S. S. Iyer, and J. A. Ott, Tech. Dig. Int. Electron Devices Meet. **91**, 25 (1991).
[2] D. C. Houghton, G. C. Aers, S. R. E. Yang, E. Wang, and N. L. Rowell, Phys. Rev. Lett. **75**, 866 (1995).
[3] M. L. W. Thewalt, D. A. Harrison, C. F. Reinhart, J. A. Wolk, and H. Lafontaine, Phys. Rev. Lett. **79**, 269 (1997).
[4] O. G. Schmidt and K. Eberl, Phys. Rev. Lett. **80**, 3396 (1998).
[5] N. L. Rowell, G. C. Aers, H. Lafontaine, and R. L. Williams, Thin Solid Films **321**, 158 (1998).
[6] S. Glutsch, D. S. Chemla, and F. Bechstedt, Phys. Rev. B **54**, 11 592 (1996).
[7] M. M. Rieger and P. Vogl, Phys. Rev. B **48**, 14 276 (1993).
[8] T. Baier, U. Mantz, K. Thonke, R. Sauer, F. Schäffler, and H. J. Herzog, Phys. Rev. B **50**, 15 191 (1994).
[9] C. Penn, P. C. M. Christianen, F. Schäffler, J. C. Maan, and G. Bauer, Physica B **256-258**, 363 (1998).
[10] D. Dutartre, G. Brémond, A. Souifi, and T. Benyattou, Phys. Rev. B **44**, 11 525 (1991).
[11] C. G. Van de Walle and R. M. Martin, Phys. Rev. B **34**, 5621 (1986).
[12] S. Glutsch, F. Bechstedt, W. Wegscheider, and G. Schedelbeck, Phys. Rev. B **56**, 4108 (1997).
[13] O. Madelung, in *Numerical Data and Functional Relationships in Science and Technology*, edited by O. Madelung, M. Schulz, and H. Weiss, Landolt-Börnstein, New Series, Vol. 17, Pt. a (Springer, Heidelberg, 1982).
[14] C. G. Van de Walle, Phys. Rev. B **39**, 1871 (1989).